Stepwise or concerted? A DFT study on the mechanism of ionic Diels–Alder reactions of chromanes

MINA HAGHDADI*, SEYEDEH SOGHRA MOUSAVI and HASSAN GHASEMNEJAD

Department of Chemistry, Islamic Azad University, P.O. Box 755, Babol branch, Babol, Iran

Abstract: The stepwise and concerted ionic Diels–Alder reactions between phenyl(pyridin-2-ylmethylene)oxonium and styrene derivatives were explored theoretically. The results support the use of a computational method *via* persistent intermediates. The DFT method was essential to reproduce a reasonable potential energy surface for these challenging systems.

Keywords: styrene; ionic Diels–Alder reaction; stepwise; concerted; DFT study; reactivity indices.

INTRODUCTION

The chromane skeleton appears in a number of natural products, such as tocopherols[1] and flavans.[2] They display a diverse array of biological activities, including antioxidant,[3] antiestrogens,[4] antiviral,[5] antihypertensive[6] and anticancer[7] activity. Common approaches to prepare the chromane skeleton[8] are Diels−Alder reactions of *o*-quinone methides (1-oxadienes),[9] additions of *O*-hydroxy acetophenones[10] and intramolecular nucleophilic substitution of phenols.[11] Alternative approaches to the chroman skeleton are of considerable interest for the formation of substituted chromanes.

Diels−Alder (DA) reactions and their formal equivalents provided a powerful means for the rapid construction of heterocyclic scaffolds. Oxa- and aza-DA variants were developed in which the dienophile and/or dienes could incorporate the heterocomponents.[12] One such aza-variant is the Povarov reaction,[13,14] originally developed 50 years ago, which has considerable utility. These DA reactions, classified as ionic DA reactions (I-DA), in which positively or negatively charged ionic species can participate in these reactions. In I-DA type of reactions, the reagents, transition states (TSs), feasible intermediates and cycloadducts remain charged during the cycloaddition reaction.[15] I-DA reactions could be classified as anionic and cationic DA reactions. However, while cationic DA reac-

tions occur rapidly at very low temperatures,[16] usually at –78 °C, due to the high electrophilic character of cationic species, there are few anionic DA reactions because, in spite of the high nucleophilic character of anionic species, these reactions do not occur easily in the absence of strong electrophiles.[17] The authors performed a series of experiments in order to establish the mechanism of these I-DA reactions.

Several theoretical studies were devoted to I-DA reactions.[18–21] The theoretical studies of Domingo *et al.* on I-DA reactions of iminium cations indicated that both one-step and stepwise mechanisms could be found.[18] The presence of the strong electron withdrawing pyridinium substituent in the iminium cation enabled the stabilization of a feasible intermediate once the first C–C single bond had completely formed, making corresponding process stepwise.[19] Recently, Batey *et al.* reported the synthesis of chromanes *via* the I-DA reaction of *O*-aryl oxonium species with some alkenes, including cyclopentene and styrene, yielding the formal [4+2] cycloadducts, which by one rapid loss of a proton afford chromanes.[22a] Their results showed that such oxonium ion species are more reactive than the corresponding iminium ions and capable of undergoing either direct
I-DA reaction or the equivalent stepwise Prins addition/intramolecular electrophilic aromatic substitution reaction to give chromans. Moreover, in 2014, a theoretical study on the mechanism of oxa-Povarov reactions was reported by Domingo *et al.*[22b] They studied the stereoselectivity of the I-DA reaction of *O*-aryl oxonium with cyclopentene and styrene at the B3LYP/6-31G* level in the gas phase and solvent, which was not in agreement with the experimental results.

In the present study, the stereoselectivity, regioselectivity and conformational analysis on the stepwise and concerted mechanism of the oxa-Povarov reaction leading to distereosynthesis of 2,4-substituted chromane[22a] were investigated by theoretical methods. In addition, the influence of substituents on styrene was analyzed in these reactions. Herein, the I-DA reactions between cationic aryl oxonium **1** and styrene derivatives **2a**–**c** are analyzed (Scheme 1) using the DFT method. Several pathways were analyzed in an attempt to elucidate the energetic difference between the stepwise mechanism and the concerted one. The calculations support the experimental finding of a two-step mechanism, as proposed by Batey *et al.*[22a] In order to evaluate fully the possible reaction pathways, several TSs and intermediates were optimized at the B3LYP/cc-pVDZ and MPWB1K/aug-cc-pVTZ level of theory.

CALCULATIONS

The ubiquitous B3LYP[23] hybrid functional has been the workhorse of quantum chemical studies on organic molecules for years.[24] It is well-known that B3LYP could describe interactions in Diels–Alder reactions. Recently, some functionals such as the MPWB1K,[22b,25] were proposed to investigate the reaction energies, barrier heights and intermediates for Diels–

–Alder reactions. For a comprehensible comparison of geometries, we were prompted to the optimization of all species in the mentioned I-DA reactions using both B3LYP and the MPWB1K exchange–correlation functional. The cc-pVDZ basis set was used for full optimization using the B3LYP method and a single point with *aug*-cc-pVTZ basis set of the MPWB1K method. Energies were then recalculated at the MPWB1K/aug-cc-pVTZ level, using the polarizable continuum model (PCM) as developed by the Tomasi group[26] within the framework at the self-consistent reaction field (SCRF).[27] Dichloromethane ($\varepsilon = 8.93$) was selected as a moderately polar organic solvent. The electronic energies were corrected with ZPE at the B3LYP/cc-pVDZ level. All calculations were performed using the Gaussian 09 program.[28]

The electronic structures of the stationary points were analyzed by the natural bond orbital (NBO) method.[29] Global reactivity indexes were estimated according to the equations recommended by Parr and Yang.[30] The global electrophilicity index, ω, is given by the following expression:[31]

$$\omega = \frac{\mu^2}{2\eta} \tag{1}$$

where μ is the electronic chemical potential and η is the chemical hardness. Both quantities may be approached in terms of the one-electron energies of the frontier molecular orbitals HOMO and LUMO, ε_H and ε_L, respectively:[32]

$$\mu = \frac{\varepsilon_H + \varepsilon_L}{2} \tag{2}$$

$$\eta = \varepsilon_H + \varepsilon_L \tag{3}$$

Recently, Domingo introduced an empirical (relative) nucleophilicity index,[33] based on the HOMO energies obtained within the Kohn Sham scheme,[34] that were defined as:

$$\varepsilon_{HOMO}(NU) + \varepsilon_{HOMO}(TCE) \tag{4}$$

Nucleophilicity is referred to tetracyanoethylene (TCE), because it presents the lowest HOMO energy in a large series of molecules already investigated in the context of polar cycloadditions. This choice allows a nucleophilicity scale of positive values to be conveniently handled. Recently, Domingo proposed two new electrophilic, P_k^+, and nucleophilic, P_k^-, Parr functions based on the atomic spin density distribution at the radical anion and cation of a neutral molecule.[35] The electrophilic, P_k^+, and nucleophilic, P_k^-, Parr functions were obtained through the analysis of the Mulliken atomic spin density of the radical anion and cation by single-point energy calculations over the optimized neutral geometries using the unrestricted UB3LYP formalism for radical species. The local electrophilicity indices, ω_k,[36] and the local nucleophilicity indices, N_k,[34] were calculated using the following expressions:

$$\omega_k = \omega P_k^+ \tag{5}$$

$$N_k = N P_k^- \tag{6}$$

where P_k^+ and P_k^- are the electrophilic and nucleophilic Parr functions,[35] respectively.

RESULTS AND DISCUSSION

Experimentally, two concerted and a stepwise mechanism were suggested for these I-DA reactions of which the stepwise mechanism may be preferred to

the concerted,[22a] because the reaction is not stereospecific with respect to alkene geometry and the oxa-Povarov reaction must proceed through stepwise pathways.

Therefore, two possible mechanisms for these reactions, concerted and stepwise mechanism were investigated herein to evaluate the energy differences between them by theoretical methods. Then, the present study was divided into three parts: first, a mechanistic study of the I-DA reactions of (*E*)-phenyl(pyridin-2-ylmethylene)oxonium (**1**) and styrene derivatives **2a**–**c**, to yield the chromane derivatives **7**–**10**, was performed along the concerted and stepwise mechanisms. Thereafter, an analysis of the geometrical and electronic structure of the stationary points was undertaken and finally, an analysis of the DFT reactivity indices of the reactants was performed.

I) Study of I-DA reaction of (E)-phenyl (pyridin-2-ylmethylene)oxonium (1) and the styrene derivatives 2a–c along the concerted mechanism

The reaction of aryl oxonium **1** species and styrene derivatives **2a**–**c** comprises two consecutive steps (Scheme 1): *i*) an I-DA reaction between **1** and **2a**–**c** to yield the corresponding intermediates **3**–**6** and *ii*) the elimination of hydrogen to give chromans **7**–**10**. The relative energies and Gibbs free energies for the stationary points are given in Table I, and Table S-I of the Supplementary material to this paper.
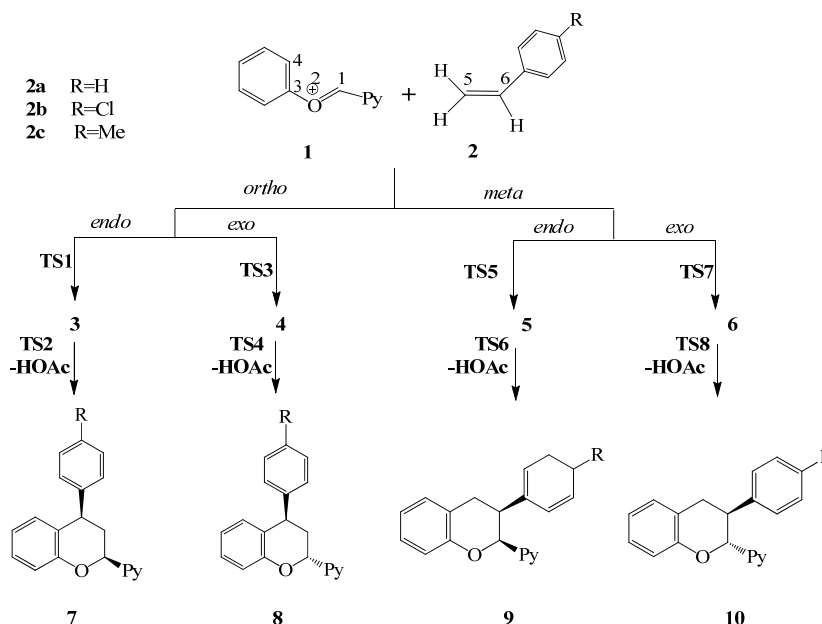
Scheme 1. The calculated possible reaction pathways for the concerted mechanism of the I-DA reaction between phenyl (pyridin-2-ylmethylene)oxonium (**1**) and styrene derivatives **2a**–**c**.

TABLE I. The calculated activation energies ($\Delta E^{\#}$), activation free energies ($\Delta G^{\#}$) and reaction energies (ΔE_r), all in kJ mol^{-1}, of the I-DA reactions between phenyl(pyridin-2-ylmethylene)oxonium (**1**) and styrene derivatives **2a–c** for the concerted mechanism (for a full comparison of energies see the Supporting material)

Species	TS	$\Delta E^{\#a}$	$\Delta E^{\#b}$	$\Delta G^{\#a}$	ΔE_r^{a}	ΔE_r^{b}
1+2a→3a-*endo*	**TS1a**	15.12	–10.29	67.95	–87.26	–174.75
3a→7a-*endo*	**TS2a**	–75.23	–163.30	–12.55	–261.17	–328.57
1+2a→4a-*exo*	**TS3a**	14.10	–9.13	66.00	–88.14	–179.91
4a→8a-*exo*	**TS4a**	–63.76	–146.07	–0.39	–245.93	–313.21
1+2b→3b-*endo*	**TS1b**	21.21	–2.55	72.74	–78.60	–165.50
3b→7b-*endo*	**TS2b**	–74.93	–162.44	–10.71	–261.36	–337.05
1+2b→4b-*exo*	**TS3b**	20.59	–1.95	72.31	–79.26	–170.15
4b→8b-*exo*	**TS4b**	–64.83	–147.09	–1.32	–246.50	–322.51
1+2c→3c-*endo*	**TS1c**	5.53	–16.39	55.63	–90.62	–178.37
3c→7c-*endo*	**TS2c**	–74.66	–163.47	–10.23	–260.63	–337.13
1+2c→4c-*exo*	**TS3c**	4.27	–17.67	61.47	–91.68	–182.74
4c→8c-*exo*	**TS4c**	–63.22	–145.42	0.30	–245.17	–321.63

[a]Optimization was performed at the B3LYP/cc-pVDZ level of theory; [b] calculated at MPWB1K/*aug*-cc--pVTZ//B3LYP/cc-pVDZ level

Due to the asymmetry of the two reagents, four competitive pathways are feasible for the I-DA reaction between aryl oxonium ion **1** and styrene derivatives **2a–c**. They are related to the two stereoisomers corresponding to the *endo* and *exo* approach modes of the styrene aryl group relative to the phenyl group of the oxonium ion, and the two regioisomeric possibilities, *ortho* and *meta* (Scheme 1). **TS1**, **TS3**, **TS5** and **TS7** were used to indicate the transition states (TSs) of the first step, **TS2**, **TS4**, **TS6** and **TS8** are the TSs for the second step, **3–6** are intermediates and **7–10** are cycloadducts of each pathway. The structures of the TSs and intermediates are displayed in Figs. S-1–S-3 of the Supplementary material.

As can be seen from the results of the calculations presented in Tables I and S-I, the transition states of the first step (cycloaddition reaction), **TS1**, **TS3**, **TS5** and **TS7**, are more energetic than the second step (elimination of a proton), **TS2**, **TS4**, **TS6** and **TS8**, which suggests that the cycloaddition step is the rate-determining step. Then in *ortho-endo* pathway, the energy barriers for two transition states, **TS1a** and **TS2a** are 15.12 and –75.23 kJ mol^{-1} for the B3LYP geometries, and –10.29 and –163.30 kJ mol^{-1} for the MPWB1K geometries, respectively, and the first step with **TS1a** could be the rate-controlling one. The energy barriers of the first step for *ortho* and *meta* pathways are 15.12, 14.10, 42.10 and 59.85 kJ mol^{-1} for the B3LYP geometries, and –10.29, –9.13, 19.20 and 31.81 kJ mol^{-1} for the MPWB1K geometries, respectively, which are higher than of the second steps and the intermediate **3a** with –87.26 kJ mol^{-1} could be a stable compound.

In order to obtain a quantitative estimate of the conformational energies in such systems, conformational analyses of the chromane ring were performed for

intermediates in all pathways at B3LYP/cc-pVDZ level, which adopts two conformers, distorted half-chair and boat conformations. The conformational analysis showed that the distorted boat conformers are more stable than the chair conformers for the *ortho-endo* and *meta-endo* pathways by 16.73 and 27.28 kJ mol^{-1}, respectively, while in the *ortho-exo* and *meta-exo* pathways, the distorted chair conformers are the more stable ones by 15.21 and 11.33 kJ mol^{-1}, respectively.

Similar to the *ortho-endo* pathway, a common intermediate, **4a**, is formed in the *ortho-exo* pathway, *via* **TS3a** with an energy barrier of 14.10 kJ mol^{-1} at the B3LYP/cc-pVDZ and –9.13 at the MPWB1K/*aug*-cc-pVTZ level. Then, **4a** loses a proton (as AcOH) to form the cycloadduct of **8a** *via* **TS4a**, the barrier height of which is –63.76 kJ mol^{-1} at the B3LYP method and –146.0 kJ mol^{-1} at the MPWB1K method (in Fig. S-1, AcO^{-} is not shown in all structures but it was considered in all of the calculations). As mentioned above, the energy barrier of the *ortho-endo* pathway is lower than those of the others are, and should be the most favorable pathway from the kinetic viewpoint.

The processes are extremely exothermic and the corresponding cyclo-adducts, **7a** and **8a**, are stable because their energies are lower than their corresponding reactants by –261.17 and –245.93 kJ mol^{-1} with B3LYP calculations, and –328.57 and –313.21 kJ mol^{-1} with MPWB1K calculations, respectively. The most favorable product **7a** was also confirmed, suggesting that the *ortho--endo* pathway is the favorable pathway from the thermodynamic viewpoint. The transition states of the *meta* pathways, **TS5a**, **TS6a, TS7a** and **TS8a**, have higher energy than those of the *ortho* ones, indicating that the *ortho* pathways are expected to be the dominant reaction pathways. Therefore, the *meta* pathways were ignored due to their high potential energies and focus was directed to the *ortho* pathways, see more information about *meta* pathways in Table S-I and Fig. S-3 of the Supplementary material.

To understand the effects of electron donating (methyl) and electron withdrawing (chloro) substituents (chloro) on the styrene ring on the I-DA reaction, the reactions of the aryloxonium ion **1** with 4-chlorostyrene (**2b**) and 4-methylstyrene (**2c**) were investigated. These two I-DA reactions also take place in the same way as mentioned earlier (I-DA reaction of **1+2a**). Then, the two *ortho* pathways dominated the reaction pathways.

As shown in Table I, along the *ortho* pathway, the chloro group on styrene slightly increased the activation energies of **TS1** and **TS3**, while the methyl group decreased the energy barriers (10 kJ mol^{-1}), relative to the parent (styrene). The activation energies associated to the regioisomeric pathways (*ortho* and *meta*) indicated a large regioselectivity in the I-DA reaction of **1** with **2b** and **2c**. Thus in this section, for the I-DA reactions of **1** with **2b** and **2c**, the main focus

was on the two *ortho* pathways and *meta* ones were ignored due to the high potential energies (Tables I and S-I).

If the easy equilibrium between all stereoisomers is considered, the most favorable reaction pathway corresponds to the formation of **7c** *via* **TS1c**, by 5.53 kJ mol^{-1} at the B3LYP level and -16.39 kJ mol^{-1} at the MPWB1K level.

A comparison of the activation energies for all the I-DA reactions indicated that the energy of the transition states associated with the *ortho-endo* pathway were slightly lower than those of the *ortho-exo* ones; which is in agreement with the experimental results.[22] When the solvent effects of CH_2Cl_2 were considered, the activation energies increased. For example, the activation barrier for the first step of the I-DA reaction of **1** with **2a** becomes 15.52 kJ mol^{-1} with MPWB1K calculations, which is 25.81 kJ mol^{-1} higher than that in gas phase (-10.29 kJ mol^{-1}). In addition, the relative energy of **3a** is reduced (by about 30 kJ mol^{-1}) in gas phase, which shows that it becomes more stable than in the solvent. Furthermore, the predicted stereoselectivity in the solvent remains almost the same as in the gas phase (the *ortho-endo* pathway is preferred). Thus, it is apparent that in this work geometry optimization in the continuum solvent does not offer any direct advantage over the single-point calculations on the gas phase geometries.

II) Study of I-DA reaction of (E)-phenyl(pyridin-2-ylmethylene)oxonium (**1**) and the styrene derivatives **2a**–**c** along the stepwise mechanism

Experimentally, these reactions were not stereospecific with respect to the alkene geometry and scrambling was observed, thus the oxa-Povarov reaction must proceed through a stepwise path. Hence, the second suggested mechanism is a stepwise one. The TSs structures, suggested intermediates, products and related energies are provided in Scheme 2, Table II and Table S-II of the Supplementary material.

The computational results indicated that these I-DA reactions could be achieved by a stepwise mechanism along four competitive pathways, two stereoselective (*endo* and *exo*) and two regioselective pathways (*ortho* and *meta*). The initial stepwise Prins-type addition of the styrene derivatives **2a**–**c** to the oxonium **1** generates carbocation intermediates, **11**, **14**, **17** and **20** *via* **TS9**, **TS13**, **TS17** and **TS21**. The relative stereochemistry of the C_1–C_5 or C_1–C_6 bond formation could be compared to the addition of styrene to the oxonium ion. The computational study revealed that I-DA reactions between styrene derivatives and the oxonium ion occurred preferentially to give the *syn* carbocation intermediate. These observations were rationalized comparing the energy barriers of all TSs, of which the lowest energy barrier as starting points were predicted for **TS9** or **TS13** in the *ortho* pathways. Next, the newly attached bond C–C undergoes a rotation to form **12, 15, 18** and **21** *via* **TS10**, **TS14**, **TS18** and **TS22**. Then a rotation along the newly formed σ bond in the intermediates yields new inter-

mediates **13**, **16**, **19** and **22** *via* **TS11**, **TS15**, **TS19** and **TS23**, respectively. Now, the latter intermediates having the proper stereochemistry undergo Friedel−Crafts cyclization to form **3**–**6** *via* **TS12**, **TS16**, **TS20** and **TS24**, respectively.
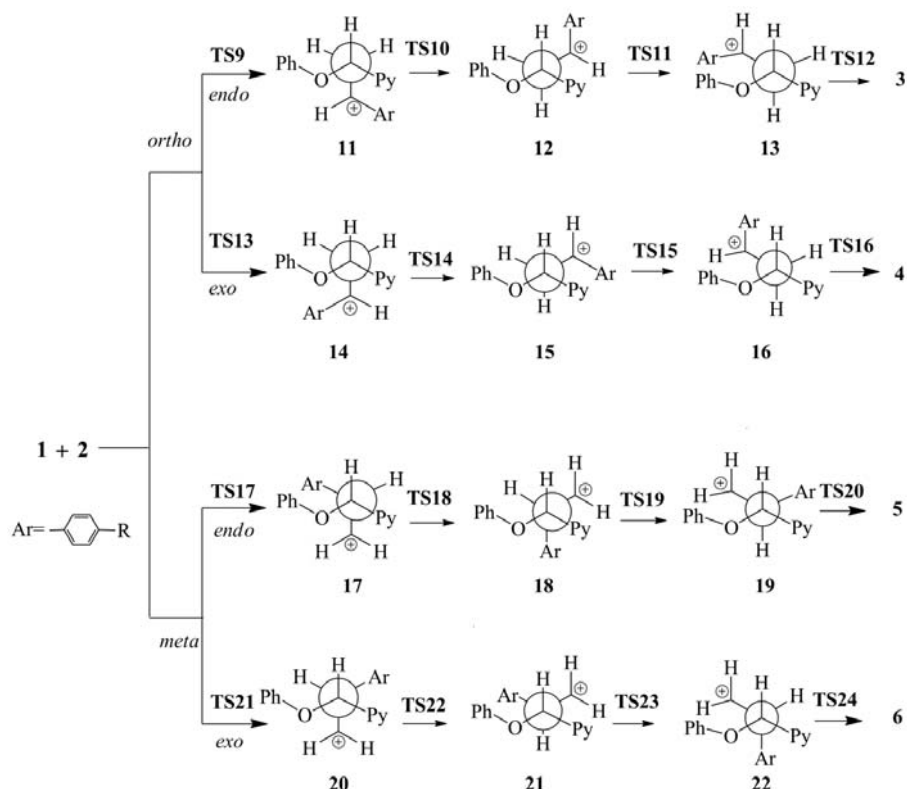
Scheme 2. The calculated possible reaction pathways for the stepwise mechanism of the I-DA reaction between phenyl(pyridin-2-ylmethylene)oxonium (**1**) and the styrene derivatives **2a**–**c**.

A comparison among the activation energies and reaction energies for the I-DA reaction of **1** with **2a** in Table II and Table S-II of the Supplementary material indicated that the *meta* pathways with extremely high potential energies should be ignored and thus attention was focused on the *ortho* pathways of these reactions. For more information about the *meta* pathways, see Table S-II of the Supplementary material.

In *ortho-endo* stepwise pathway, first, styrene **2a** approaches to **1** through a synclinal orientation to generate the carbocation intermediate **11a** *via* **TS9a**. The energy barrier for this process is −7.26 kJ mol^{-1} at the B3LYP level and −29.93 kJ mol^{-1} at the MPWB1K level with **11a** being more stable than reactants by −37.44 kJ mol^{-1} according to the B3LYP method and −89.52 kJ mol^{-1} according

to the MPWB1K method. Then intermediate **11a** must undergo C_1–C_5 bond rotation to generate intermediate **12a**, which is antiperiplanar, *via* **TS10a** with an energy barrier of −35.41 and −79.85 kJ mol^{-1} at the B3LYP and MPWB1K levels, respectively. Next, **12a** undergoes rotation around the same C_1–C_5 bond, with an energy cost of −16.45 kJ mol^{-1} (−61.79 kJ mol^{-1} at the MPWB1K level), to yield **13a** *via* **TS11a**. Subsequently, intermediate **13a** undergoes Friedel−Crafts cyclization to produce **3a** *via* **TS12a**. Finally, **3a** loses a proton to produce **7a**, as discussed in the concerted section.

TABLE II. The calculated activation energies ($\Delta E^{\#}$), activation free energies ($\Delta G^{\#}$) and reaction energies (ΔE_r), all in kJ mol^{-1}, of the I-DA reactions between phenyl(pyridin-2-yl-methylene)oxonium (**1**) and styrene derivatives **2a–c** for the stepwise mechanism (for a full comparison of the energies, see the Supplementary material)

Species	TS	$\Delta E^{\#a}$	$\Delta E^{\#b}$	$\Delta G^{\#a}$	$\Delta E_r{}^a$	$\Delta E_r{}^b$
1+2a→11a-*endo*	**TS9a**	−7.62	−29.93	42.44	−37.44	−89.52
11a→12a-*endo*	**TS10a**	−35.41	−79.85	30.39	−45.68	−91.18
12a→13a-*endo*	**TS11a**	−16.45	−61.79	43.93	−33.65	−79.52
13a→3a-*endo*	**TS12a**	−21.46	−75.72	40.28	−87.26	−174.75
1+2a→14a-*exo*	**TS13a**	−5.85	−28.31	45.58	−35.77	−88.96
14a→15a-*exo*	**TS14a**	−18.58	−68.66	42.02	−72.32	−118.12
15a→16a-*exo*	**TS15a**	−6.05	−56.07	53.42	−28.89	−75.91
16a→4a-*exo*	**TS16a**	−14.30	−63.82	51.15	−88.14	−179.91
1+2b→11b-*endo*	**TS9b**	−1.66	−23.56	47.84	−33.95	−84.80
11b→12b-*endo*	**TS10b**	−29.54	−72.84	36.64	−42.07	−86.83
12b→13b-*endo*	**TS11b**	−13.33	−57.43	47.45	−25.55	−71.62
13b→3b-*endo*	**TS12b**	−15.36	−69.28	46.97	−78.60	−165.50
1+2b→14b-*exo*	**TS13b**	0.015	−21.41	51.45	−13.27	−85.59
14b→15b-*exo*	**TS14b**	−15.05	−64.25	46.18	−67.30	−112.17
15b→16b-*exo*	**TS15b**	7.09	−32.38	70.46	−25.68	−71.94
16b→4b-*exo*	**TS16b**	−8.425	−56.87	29.67	−79.26	−170.15
1+2c→11c-*endo*	**TS9c**	−17.29	−38.26	32.19	−53.23	−106.06
11c→12c-*endo*	**TS10c**	−50.56	−95.89	15.68	−65.38	−112.65
12c→13c-*endo*	**TS11c**	−38.12	−84.02	22.37	−53.65	−101.37
13c→3c-*endo*	**TS12c**	−35.06	−90.43	27.30	−90.62	−178.37
1+2c→14c-*exo*	**TS13c**	−15.12	−35.15	35.51	−56.49	−110.39
14c→15c-*exo*	**TS14c**	−39.28	−91.24	22.13	−88.39	−135.34
15c→16c-*exo*	**TS15c**	−16.54	−59.82	46.21	−50.10	−101.07
16c→4c-*exo*	**TS16c**	−27.07	−79.41	37.93	−91.68	−182.74

[a]Optimization was performed at B3LYP/cc-pVDZ level of theory; [b]calculated at the MPWB1K/*aug*-cc-pVTZ//B3LYP/cc-pVDZ level

From a comparison of the relative energies of the TSs and intermediates in the *ortho-endo* stepwise pathway, some results could be concluded as follows: *i*) the formation of the C_1–C_5 bond (**TS9a**) is the rate-determining step, *ii*) as expected, the energy of intermediates are low compared to the surrounding barriers (**TS9a–TS12a**), *iii*) the low energy of the TSs and intermediates (their ener-

gies are lower than those of reactants) together with the rotation of the C_1–C_5 bond may suggest that these processes occur *via* an reversible stepwise mechanism, *iv*) furthermore, the lowest activation and relative energies were seen for **TS10a** and **3a**, respectively. The optimized geometries of TSs and intermediates involved in the domino pathway are given in Figs. S-2 and S-3 of the Supplementary material, respectively.

Similar results were obtained for the *ortho-exo* pathway, which are given in Table II. Comparing the *ortho* pathways with regard to stereochemistry, the *endo* pathways are usually followed preferentially, as the activation energies in the more stable step (**TS10a**) are slightly lower than those in the *exo* addition and the resulting intermediates are more stable. These results confirmed that the *ortho--endo* pathway is the most energetically favorable one among the other proposed reaction pathways, in agreement with the experimental results.

Moreover, the stepwise pathways were investigated in I-DA reaction of 4-chlorostyrene and 4-methylstyrene (**2b** and **2c**, respectively) with aryl oxonium ion **1** (Scheme 2) along the more favored pathways (*ortho* ones), and the results of their activation energies and reaction energies, given in Table II, indicated that the *ortho-endo* pathways are the more favorable ones.

The theoretical results proved that the I-DA reaction with the lowest activation barriers involved 4-methyl substituted styrene along the *ortho-endo* pathway, while 4-chloro substitution increased the activation and reaction energies.

As can be seen in Table II, the activation energies varied within the series of dienophiles. Of all the possible stepwise TSs, **TS10** is consequently favored over the others. Furthermore, the energy of TSs increased when going from **2a** to **2b** and became the lowest for **2c**. A similar trend was observed for their intermediates, *i.e.*, **11c**, **12c**, **13c** and **3c** are the most stable intermediates, while the intermediates of I-DA reaction **1**+**2** appear to be less stable.

III) Geometrical parameters

Selected geometry parameters of the **TS**s on the concerted pathways at the B3LYP/cc-pVDZ level are shown in Fig. 1. As can be seen, the lengths of the C_1–C_5 and C_4–C_6 bonds (the atom numbering is given in Scheme 1) for the concerted mechanism, at the *ortho-endo* pathway (**TS1**), are about 2.23 and 3.89 Å, and at the *ortho-exo* (**TS3**), the corresponding values are 2.25 and 3.89 Å, respectively. These bond lengths indicated that both TSs structures are with highly asynchronous bond formation processes, where it seems only the C_1–C_5 bond is being formed.

The extent of bond-formation along a reaction pathway is provided by the concept of bond order (BO).[37] The BO values of the C_4–C_6 forming bonds for the concerted mechanism along the most favorable pathway is virtually zero, indicating a stepwise or at least highly asynchronous pathway for these reactions.

The polar nature of the two cyclization modes can be estimated by a charge transfer (CT) analysis at the TSs.[29] The CT descriptors (Figs. S-1 and S-3) clearly show that these reactions are polar according to the Domingo classification.

Moreover, the important dihedral angles and bond lengths for the **TS**s and intermediates of stepwise mechanism are presented in Table III, and Table S-III of the Supplementary material.

TABLE III. Selected geometrical parameters, bond lengths (r / Å) and dihedral angles (φ / °) for the stationary points of I-DA reactions between phenyl(pyridin-2-ylmethylene)oxonium (**1**) and styrene (**2a**) for the *ortho* pathway of stepwise mechanism at the B3LYP/cc-pVDZ level of theory[a] (for numbering of atoms, see Scheme 2, and for full comparison of geometrical parameters, see the Supporting information to this paper)

Species	$\varphi_{O-C1-C5-C6}$	r_{C1-O}	r_{C3-C4}	r_{C4-C6}	r_{C5-C6}
1	–	1.28	1.39	–	–
2a	–	–	–	–	1.34
TS9a	69.15	1.31	1.39	4.93	1.37
11a	53.52	1.41	1.39	5.09	1.47
TS10a	116.23	1.43	1.39	5.74	1.48
12a	172.26	1.41	1.40	5.22	1.46
TS11a	115.01	1.44	1.39	4.93	1.45
13a	45.23	1.43	1.40	4.59	1.47
TS12a	65.20	1.45	1.44	4.51	1.48
3a	26.11	1.48	1.47	1.58	1.55
TS2a	49.10	1.46	1.48	1.58	1.55
7a	62.05	1.43	1.40	1.52	1.54
TS13a	67.86	1.30	1.39	4.55	1.37
14a	60.11	1.40	1.39	5.13	1.47
TS14a	120.32	1.42	1.39	5.52	1.47
15a	177.17	1.40	1.40	4.43	1.46
TS15a	119.75	1.42	1.40	4.89	1.46
16a	41.30	1.42	1.39	4.72	1.47
TS16a	45.52	1.45	1.44	2.49	1.49
4a	53.14	1.47	1.49	1.55	1.54
TS4a	44.33	1.46	1.49	1.57	1.55
8a	53.81	1.43	1.40	1.52	1.54

CONCLUSION

The molecular mechanism of I-DA reactions between aryl oxonium **1** species and styrene derivatives **2a**–**c** yielding chromanes **7**–**10** was studied using the DFT method at the B3LYP/cc-pVDZ level of theory.

The formation of cycloadducts **7**–**10** occurs through two consecutive steps; first, a cycloaddition reaction between **1** and **2a**–**c** occurred to yield the intermediates **3**–**6**, then the elimination of hydrogen from these intermediates yielding

chromanes **7**–**10**. These I-DA reactions are completely regioselective and slightly *endo* selective.

The calculation results suggest that:

I. The elimination of hydrogen is kinetically favored over the cycloaddition process (first step).

II. The concerted and stepwise mechanism of all the I-DA reactions were investigated, the results of which showed that the stepwise mechanism is more favorable than the concerted ones.

III. The *ortho-endo* pathway with an energy barrier of 15.12 kJ mol^{-1} for 4-Cl styrene and 5.53 kJ mol^{-1} for 4-Me styrene, on the concerted mechanism is the most energetically favorable pathway; on the stepwise mechanism these energy barriers are reduced to –13.33 and –38.12 kJ mol^{-1}, respectively.

IV. DFT-based reactivity indices clearly predict the regiochemisty of the isolated cycloadducts.

Moreover, it is reasonable to conclude that the gas-phase geometry optimization at the B3LYP/cc-pVDZ level can give quite good estimates of the mechanism and stereoselectivity in I-DA reactions.

SUPPLEMENTARY MATERIAL

The calculated energies, geometrically optimized transition states and intermediates, as well as selected geometrical parameters are available electronically from http:////www.shd.org.rs/JSCS/, or from the corresponding author on request.

И З В О Д

ПОСТЕПЕНО ИЛИ КОНЦЕРТОВАНО? DFT СТУДИЈА МЕХАНИЗМА ЈОНСКЕ ДИЛС–АЛДЕРОВЕ РЕАКЦИЈЕ ХРОМАНА

MINA HAGHDADI, SEYEDEH SOGHRA MOUSAVI и HASSAN GHASEMNEJAD

Department of Chemistry, Islamic Azad University, P.O. box 755, Babol branch, Babol, Iran

Постепене и концертоване јонске Дилс–Алдерове рекције између фенил(пиридин--2-илметилен)оксонијумских и стиренских деривата изучаване су коришћењем теоријских метода. Резултати дају подршку употреби рачунарких метода првенствено на стабилнијим интермедијерима. DFT метод се показао битним за репродуковање реалистичне површине потенцијалне енергије за ове захтевне системе.

(Примљено 20. априла, ревидирано 26. септембра, прихваћено 5. октобра 2015)

REFERENCES

1. A. KamaI-Eldin, L. A. Appelqvist, *Lipids* **31** (1996) 671
2. A. R. Tapas, D. M. Sakarkar, R. B. Kakde, *Trop. J. Pharm. Res.* **7** (2008) 1089
3. a) E. J. Jacobsen, F. J. Van Doornik, D. E. Ayer, K. L. Belonga, J. M. Braughler, E. D. Hall, D. J. House, *J. Med. Chem.* **35** (1992) 4464; b) K. Terao, E. Niki, *J. Free Rad. Biol. Med.* **2** (1986) 193; c) J. M. Grisar, M. A. Petty, F. N. Bolkenius, J. Dow, J. Wagner, E. R. Wagner, K. D. Haegele, W. D. Jong, *J. Med. Chem.* **34** (1991) 257
4. J. Lal, *Contraception* **81** (2010) 275

5. Y. Kashiwada, K. Yamazaki, Y. Ikeshiro, T. Yamagishi, T. Fujioka, K. Mihashi, K. Mizuki, L. M. Cosentino, K. Fowke, S. L. Morris-Natschke K.-H. Lee, *Tetrahedron* **67** (2001) 1563

6. F. Cassidy, J. M. Evans, M. S. Hadley, A. H. Haladij, P. E. Leach, G. Stemp, *J. Med. Chem.* **35** (1992) 1623

7. a) C. Pouget, C. Fagnere, J. P. Basly, H. Leveque, A. J. Van Doornik, *Tetrahedron* **56** (2000) 6047; b) N. P. Seeram, H. Jacobs, S. McLean, W. F. Reynolds, *Phytochemistry* **49** (1998) 1389

8. H. C. Shen, *Tetrahedron Lett.* **65** (2009) 3931

9. a) R. W. Van de Water, T. R. R. Pettus, *Tetrahedron Lett.* **58** (2002) 5367; b) K. A. Korthals, W. D. Wulff, *J. Am. Chem. Soc.* **130** (2008) 2898; c) T. Inoue, S. Inoue, K. Sato, *Bull. Chem. Soc. Jpn.* **36** (1990) 1647

10. S. K. Ko, H. J. Jang, E. Kim, S. B. Park, *Chem. Commun.* **28** (2006) 2962

11. a) P. Kotame, B. C. Hong, J. H. Liao, *Tetrahedron Lett.* **50** (2009) 704; b) X. Meng, Y. Huang, H. Zhao, P. Xie, J. Ma, R. Chen, *Org. Lett.* **11** (2009) 991; c) N. R. Mente, J. D. Neighbors, D. F. Wiemer, *J. Org. Chem.* **73** (2008) 7963

12. a) V. M. Cherkasov, N. A. Kapran, *Chem. Heterocycl. Compd.* **28** (1992) 1101; b) K. C. Nicolaou, S. A. Snyder, T. Montagnon, G. Vassilikogiannakis, *Angew. Chem. Int. Ed.* **41** (2002) 1668

13. a) V. I. Grigos, L. S. Povarov, B. M. Mikhailov, *Russ. Chem. Bull. Int. Ed. (Engl. Transl.)* **12** (1965) 2163; b) L. S. Povarov, V. I. Grigos, B. M. Mikhailov, *Russ. Chem. Bull., Int. Ed. (Engl. Transl.)* **1** (1966) 144

14. For reviews on the Povarov reaction, see: a) L. S. Povarov, *Russ. Chem. Rev.* **36** (1967) 656; b) V. A. Glushkov, A. G, Tolstikov, *Russ. Chem. Rev.* **2** (2008) 137; c) V. V. Kouznetsov, *Tetrahedron* **65** (2009) 2721

15. L. R. Domingo, J. A. Saez, *Org. Biomol. Chem.* **7** (2009) 3576

16. a) D. G. Gassman, D. A. Singleton. *J. Org. Chem.* **51** (1986) 3075; b) P. G. Gassman, D. A. Singleton, *J. Am. Chem. Soc.* **109** (1987) 2182

17. M. V. Basaveswara Rao, J. Satyanarayana, H. Ham, H. Junjappa, *Tetrahedron Lett.* **36** (1995) 3385

18. L. R. Domingo, *J. Org. Chem.* **66** (2001) 3211

19. L. R. Domingo, M. Oliva, J. Andres, *J. Org. Chem.* **66** (2001) 6151

20. L. R. Domingo, M. Oliva, J. Andres, *J. Mol. Struct. THEOCHEM* **544** (2001) 79

21. H. Mayr, A. R. Ofial, J. Sauer, B. Schmied, *Eur. J. Org. Chem.* (2000) 2013

22. a) A. Batey, R. R. Rivka, *J. Org. Chem.* **78** (2013) 1404; b) L. R. Domingo, M. J. Aurell, P. Pérez, *RSC Adv.* **4** (2014) 16567

23. a) A. D. Becke, *Phys. Rev., A* **38** (1988) 3098; b) C. Lee, W. Yang, R. G. Parr, *Phys. Rev., B* **37** (1988) 785

24. L. Simon, J. M. Goodman, *Org. Biomol. Chem.* **9** (2011) 684

25. L. R. Domingo, M. J. Aurell, P. Pérez. *Tetrahedron* **70** (2014) 4519

26. a) J. Tomasi, M. Persico, *Chem. Rev.* **94** (1994) 2027; b) B. Y. Simkin, I. Sheikhet, *Quantum chemical and statistical theory of solutions – A computational approach*, Ellis Horod, London, 1995

27. a) E. Cances, B. Mennucci, J. Tomasi, *J. Chem. Phys.* **107** (1997) 3032; b) M. Cossi, V. Barone, R. Cammi, J. Tomasi, *Chem. Phys. Lett.* **255** (1996) 327

28. *Gaussian 09 revision A,* Gaussian, Inc., Wallingford, CT, 2009

29. A. E. Reed, R. B. Weinstock, F. Weinhold, *J. Chem. Phys.* **83** (1985) 735

30. R. G. Parr, W. Yang, *Density functional theory of atoms and molecules*, Oxford Univ. Press, New York, 1989, p. 16
31. R. G. Parr, L. Von Szentpaly, S. Liu, *J. Am. Chem. Soc*. **121** (1999) 1922
32. R. G. Parr, R. G. Pearson, *J. Am. Chem. Soc.* **105** (1983) 7512
33. L. R. Domingo, P. Pérez, *J. Org. Chem.* **73** (2008) 4615
34. P. Pérez, L. R. Domingo, M. Duque-Noreña, E. Chamorro, *J. Mol. Struct. THEOCHEM* **895** (2009) 86
35. L. R. Domingo, P. Pérez, J. A. Saez, *RSC Adv.* **3** (2013) 1486
36. L. R. Domingo, M. J. Aurell, P. Pérez, *J. Phys. Chem., A* **106** (2002) 6871
37. K. B. Wiberg, *Tetrahedron* **24** (1968) 1083
38. H. Chemouri, S. M. Mekelleche, *Int. J. Quantum. Chem*. **112** (2012) 2294
39. W. Benchouk, S. M. Mekelleche, B. Silivi, M. J. Avrell, L. R. Domingo, *J. Phys. Org. Chem*. **24** (2011) 611.